Chem. Phys. Lett.

Formation of nanostructures of hexaphenylsilole with enhanced color-tunable emissions

Chetan Jagdish Bhongale,[a] Chih-Wei Chang,[a] Eric Wei-Guang Diau,[a,*] Chain-Shu Hsu[a,*]

Yongqiang Dong,[b] and Ben-Zhong Tang[b]

[a]*Department of Applied Chemistry, Institute of Molecular Science and Center for Interdisciplinary Molecular Science, National Chiao Tung University, Hsinchu, Taiwan*

[b]*Department of Chemistry, The Hong Kong University of Science and Technology, Clear Water Bay, Kowloon, Hong Kong, P R China*

*Corresponding author. FAX:+886-3-572-3764; E-mail: diau@mail.ac.nctu.edu.tw

Abstract

Nanostructures of 1,1,2,3,4,5-hexaphenylsilole (HPS) of various types were obtained on simple reprecipitation with THF as solvent and water as non-solvent. The formation and evolution of these nanostructures were monitored with scanning electron microscopy. Using picosecond time-correlated single-photon counting, we observed enhanced emission and fluorescence lifetimes at volume fractions 70–90 % of added water. We report the first enhanced color-tunable emissions of a conjugated organic compound (HPS) due to the formation of nanoflowers, nanoglobules and microglobules, and provide time scales for those nanostructures and the corresponding intermolecular interactions in the aggregates.

1. Introduction

Organic nanoparticles have attracted much research interest because their special properties lie between the properties of molecules and those of bulk material [1]. Reprecipitation has become a popular technique to prepare nanoparticles because its operation is easy and versatile [2]. To fabricate and to investigate organic nanoparticles with varied structures, various shapes and diverse sizes has become a topic of intense research interest, as these nanostructures possess varied physicochemical properties such as luminescence [3] or large nonlinear optical efficiency [4,5]; they are thus expected to serve as novel functional materials in electronics and photonics [6]. These varieties of nanostructures are achievable on varying experimental conditions such as temperature, precipitation or aging time, and adding a template or a stabilizer [7,8]. Nakanishi and co-workers pioneered investigation of this subject, particularly focusing on fabrication of nanocrystals and characterization of organic systems [9-11].

Many conjugated organic light emitters are highly emissive in their dilute solutions but their luminescence becomes quenched when fabricated into thin films [12]. The cause of this quenching is believed to be formation of aggregates; in the solid state, the molecules aggregate to form less emissive species such as excimers, leading to luminescence with diminished efficiency [13]. Enhancement due to aggregate-induced emission (AIE) has, however, been reported for organic systems including CN-MBE [2], *p*-BSP [14], PPB [15], silole derivatives [16-22] and conjugated polymers [23]. Silole molecules such as hexaphenylsilole (HPS) are compounds in a class that exhibit weak luminescence or no luminescence in solutions but become highly emissive in their aggregates, thus making them promising materials for electroluminescence (EL)

applications [16-22]. This novel AIE effect has been rationalized to reflect the restricted intramolecular rotation of the phenyl peripheries against the silacyclopentadiene (silole) core in the nano-aggregates, thus populating the radiative state of excitons when the nonradiative channel via relaxation of vibrational and torsional energy is blocked in the aggregate state [16-18,20]. Photoluminescence (PL) of an HPS solution became enhanced on increasing the viscosity and decreasing the temperature of solutions [17,24]. Vapochromism [25] and thermochromism [26] have also been reported for HPS.

In this work, we used reprecipitation to produce nanostructures of HPS at various compositions in water and THF. The formation and growth of these nanostructures were monitored with scanning electron microscopy (SEM), steady-state absorption, PL and time-resolved emission methods. We found that the intensity of the emission attains a maximum for the 70 % solution when novel nanoflowers were produced. Although nanoflowers are formed in inorganic nano-materials [27-30], our observation with enhanced color-tunable emission of the formation of nanoflowers from conjugated organic compounds seems to be the first example discovered by simple reprecipitation.

2. Experiments

2.1 Formation of nanostructures

HPS was synthesized according to a published procedure [31]. HPS nanostructures were obtained by a simple reprecipitation method [9], in which water served as a precipitating solvent for HPS in THF. Solutions with volume fractions 0, 50, 60, 70, 80 and 90 % of water were prepared and stirred vigorously for an hour before spectral measurements. Distilled water and THF were filtered with a membrane filter (pore size

0.2 μm). In all samples, the concentration of HPS in THF solution was 1.9×10^{-5} mol L^{-1} after addition of distilled water. The resulting suspensions after water addition were homogeneous.

2.2 Characterization methods

SEM Images were acquired on a field-emission scanning electron microscope (JSM-6500 F, JEOL); to enhance the conductivity of the specimen, a layer of platinum was sputtered (current 30 mA, pressure 4 Pa, duration 30 s). UV/visible absorption spectra (Cary 50, Varian) and fluorescence spectra (F4500, Hitachi) were measured in a standard manner. Time-resolved experiments with picosecond resolution were performed with a time-correlated single-photon-counting (TCSPC) system (FluoTime 200, PicoQuant) reported elsewhere [15]. The transient data were analyzed using commercial software (FluoFit, PicoQuant). The full width at half maximum (FWHM) of the instrument response function (IRF) was determined to be ~30 ps.

3. Results and Discussion

3.1 SEM images

In four parts, Fig. 1 presents SEM photographs of HPS nanostructures prepared at (a) 60, (b) 70, (c) 80 and (d) 90 % of water. According to that evidence, the free molecules in solution began to aggregate and to evolve during growth with increasing fraction of water. Thin sheets of nanostructures of length 300–400 nm and thickness only a few nanometers were formed at 60 % volume fraction of water, initially, as the superior solvent (THF) was replaced by the inferior solvent (water) and dispersed in bulk water. As the proportion of added water was increased beyond 60 %, the molecules

aggregated to larger particles. At 70 % volume fraction of water, splendid nanoflowers were obtained, as shown in the inset of Fig. 1b. When the volume fraction of water was increased to 80 %, we observed the formation of a few nanoglobular structures along with nanoflowers (Fig. 1c). We speculate that, upon further increase of water to 80 % solution, HPS nanoglobules began to form at the expense of nanoflowers. At 90 % water, the diameter of these nanoglobules became a few micrometers. The inset of Fig. 1d shows also broken microglobules incorporated with nanosheets and nanoflowers with a surface layer of some sort, indicating that these microglobules evolved from the original nanoglobules on encapsulating those nanostructures inside globular structures at 90 % water during aging of the solution.

3.2 Absorption and emission spectra in the steady state

UV/visible absorption spectra and corresponding emission spectra of HPS with various volume fractions of water are shown in Fig. 2a and b, respectively. In general, the UV/visible spectra show absorption with a maximum near 365 nm for all solutions. The appearance of Mie scattering in the long wavelength region of the spectra for 70–90 % solutions indicates the formation of significant HPS aggregates in those solutions, which is consistent with SEM photographs shown in Fig. 1. At 70 % solution, the absorbance decreased substantially, and the maximum of absorbance shifted slightly to 370 nm. At solutions with water fractions 80 and 90 %, increased absorbance accompanied substantial Mie scattering interference shown as a tail extending into the visible region.

Notable effects were observed in the corresponding emission spectra (Fig. 2b). The HPS solution in 0–60 % water fractions showed almost no emission. Even though the

SEM image in Fig. 1a shows formation of nanosheets at 60 % water, we observed no enhancement of emission. When the water fraction was increased to 70 %, the emission became enhanced about 100 times that of the solution in pure THF, with the maximum intensity occurring at 462 nm; this enhancement is due to the formation of nanoflowers as unambiguously seen in Fig. 1b. The emission feature of a HPS film is reported to be slightly blue-shifted and narrower than that of its solution [22]. Furthermore, HPS in a mixture of acetone and water also shows a blue-shifted feature with emission enhanced at water fraction 60 % [32]. In our case, the enhanced blue-shifted spectral feature occurs at 70 % solution on formation of the novel nanoflowers.

At 80 % water, we observed a decreased PL intensity with a maximum ca. 485 nm. This decrease might be due to the formation of some nanoglobules along with nanoflowers (Fig. 1c). When the volume fraction of water was increased to 90 %, the PL intensity again increased with the wavelength red-shifted to ca. 500 nm. Fig. 3 from left to right shows PL images of solutions excited at 365 nm, for 0, 70 and 90 % volume fractions of water, respectively. Color tuning with emission enhancement of HPS was thus observed upon formation of nanoflowers and microglobules. To improve our understanding of this nanostructure-induced enhancement of emission of HPS, we performed time-resolved spectral measurements on the system.

3.3 Picosecond TCSPC measurements

Time-dependent measurements of HPS in solutions of water and THF at various concentrations were performed with excitation at λ_{ex} = 375 nm and emission observed at λ_{em} = 520 nm; typical results are shown in Fig. 4, and the fitted parameters are summarized in Table 1. The fluorescence transients with water fractions less than 60 %

featured only a pulse-limited decay (~30 ps). In dilute solution of good solvent THF, HPS molecules can move freely without restriction imposed on certain intramolecular motions. Efficient nonradiative relaxation would therefore occur from the excited state of HPS via torsional motions [15], yielding depopulation of the excited state within the observed ~30 ps.

Increasing the water fraction to 70 % caused a greatly extended lifetime of the excited state (Fig. 4). Most of the transient curve is consistent with a decay coefficient ~6 ns, but the transient at the short-time range was not perfectly fitted with only a single-exponential decay function: a rapid-decay component must be included in a parallel kinetic model to obtain a reasonable fit, which yields time coefficients 0.2 ns and 6.2 ns. We deduce that the slow decay component, ~6 ns, dominating the transient produces the observed enhancement of emission at this composition of water and THF, 70 %, at which aggregation of HPS molecules to nanoflowers began (Fig. 1b). Because the HPS molecule has a distinctly nonplanar structure in the solid state with an intermolecular distance ~10 Å [21], we expect the effect of π–π stacking in the nano-aggregates to be insignificant. The efficient nonradiative relaxation of HPS that occurs in THF became inhibited due to the restriction of the intramolecular torsional motions in the nanostructures, producing the enhanced fluorescence observed for nanoflowers at 70 % solution. The existence of a rapid decay component in the transient with a relative amplitude only 27 % reflects a minor contribution for the initial phase of relaxation of HPS nanostructures and determines the time scale, τ_1 = 200 ps, for intermolecular interaction of the nanoflower aggregates.

The transient in 80 % solution (Fig. 4) displays a much more rapid kinetic feature with a tiny slow decay component, ~2 %; its decay coefficient was determined to be 6.3 ns. This decay coefficient is similar to that for the 70 % solution, τ_2 = 6.2 ns, but the contribution of the former is much smaller due to the existence of a rapid-decay component constituting a major part of the transient, which can be well characterized with two decay coefficients, 0.15 and 0.5 ns, with relative amplitudes 74 and 24 %, respectively. As there is a correlation between the observation of the growth of the rapid-decay component that diminishes the slow-decay component, we expect that efficient intermolecular interaction, τ_1 = 150 ps, is a dominant process for relaxation of excited states in nanostructures formed in the 80 % solution, which causes significant quenching of the fluorescence in those nanoaggregates (Fig. 2b). We thus assign the two slower components to be due to two distinct nanostructures: the component with lifetime τ_2 = 6.3 ns is due to nanoflowers remaining in the 80% solution, and the intermediate component with lifetime τ_3 = 0.5 ns arises from the just formed nanoglobules (Fig. 1c).

When we increased the water volume fraction to 90 %, the kinetics of the transient showed an intermediate decay feature between those of 70 % and 80 % solutions (Fig. 4). The transient was perfectly fitted with three decay parameters, yielding decay coefficients τ_1 = 0.37 ns, τ_2 = 4.3 ns and τ_3 = 1.8 ns with relative amplitudes 36 %, 18 % and 46 %, respectively. The value of τ_1 in 90 % solution is much larger than that in 80 % solution – 370 ps vs 150 ps – indicating that intermolecular interaction of the former is less efficient, and thus slower, than that of the latter. Both components τ_2 and τ_3 thus became more pronounced for 90 % than for 80 % solution. Because the nanoglobules produced in the 80 % solution evolved to form microglobules in the 90 % solution (Fig. 1), the effective

length of conjugation of HPS aggregates might be greater for the former than the latter, which is consistent with the observed emission intensity being more intense for the former than for the latter, and the emission spectrum being red-shifted to 500 nm for the 90 % solution (Fig. 2b). With support from the steady-state data, we therefore assign the major long-decay component of the transient, τ_3, to be due to microglobules formed with water added to 90 % (Fig. 1d), whereas the minor long-decay component, τ_2, is due to other nanostructures, presumably those inside broken microglobules as is unambiguously discernible in the inset of Fig. 1d.

4. Conclusion

We have prepared nanostructures of HPS of various types in solutions of water and THF using reprecipitation, and characterized their enhanced and color-tunable photophysical properties with steady-state and time-resolved spectral methods. We observed strong emission from well evolved HPS nanoaggregates, but emission from HPS in dilute THF solution was scarcely detectable. We discovered that novel nanoflowers were produced at 70 % water with blue-shifted emission, λ_{em} = 462 nm, of which the intensity increased 100 times. At 80 % solution, nanoglobular structures were formed at the expense of the nanoflowers, and the emission intensity was decreased significantly, but microglobular structures evolved from the nanoglobules at 90 % water with intermediate emission intensity at λ_{em} = 500 nm. Picosecond time-resolved fluorescence investigations yielded excited-state lifetimes 6.2, 0.5 and 1.8 ns for nanoflowers, nanoglobules and microglobules, respectively; the corresponding relaxation periods due to intermolecular interactions among HPS molecules were 200, 150 and 370

ps, respectively. The observed enhancement in aggregation-induced emission is attributed to the deactivation of nonradiative decay through restriction of intramolecular torsional motions in those nanostructures [22].

Acknowledgements

National Science Council of the Republic of China supported this project through contracts 94-2113-M-009-016 for EWGD and 94-2120-M-009-008 for CSH.

Table1: Fitted time coefficients of HPS in water/THF solutions at various concentrations.[a,b]

Time coefficients/ns	0 %	60 %	70 %	80 %	90 %
τ_1	<0.03 (1.0)	0.04 (1.0)	0.2 (0.27)	0.15 (0.74)	0.37 (0.36)
τ_2			6.2 (0.73)	6.3 (0.02)	4.3 (0.18)
τ_3				0.5 (0.24)	1.8 (0.46)

[a] The excitation wavelength was fixed at 375 nm and emission was observed at 520 nm.
[b] The numbers in parentheses are the relative amplitudes.

Captions of figures

Fig. 1 SEM images of various nanostructures of HPS obtained from suspensions of nanoparticles contained for (a) 60, (b) 70, (c) 80 and (d) 90 % volume fractions of water added to THF, respectively.

Fig. 2 (a) UV/visible absorption spectra of HPS showing the variation of absorbance with proportions of water and THF as indicated. (b) PL spectra of HPS showing the variation of fluorescent intensity for mixtures of water and THF at various proportions as indicated.

Fig. 3 Fluorescence emission of HPS (c = 1.9 × 10^{-5} mol L^{-1}) in pure THF (left), suspensions of nanoparticles in THF/water mixtures with 70 % (middle) and 90 % (right) water and excitation at 365 nm.

Fig. 4 Picosecond fluorescent transients of HPS in water and THF mixtures with various proportions as indicated. The data were obtained with excitation at λ_{ex} = 375 nm and emissions probed at λ_{em} = 520 nm.

References

[1] D. Horn, J. Rieger, Angew. Chem. Int. Ed. 40 (2001) 4330.

[2] B.-K. An, S.-K. Kwon, S.-D. Jung, S. Y. Park, J. Am. Chem. Soc. 124 (2002) 14410.

[3] H. Yoshikava, H. Masuhara, J. Photochem. Photobiol. C 1 (2000) 57.

[4] D. S. Chemla, J. Zyss, In Nonlinear Optical Properties of Organic Molecules and Crystals, Academic Press, Orlando, USA, 1987.

[5] R. J. Gehr, R. W. Boyd, Chem. Mater. 8 (1996) 1807.

[6] H. Oikawa, F. Kasai, H. Nakanishi, In Anisotropic Organic Materials, American Chemical Society, Washington, DC, 2002.

[7] H. Kasai, H. Kamatani, Y. Yoshikawa, S. Okada, H. Oikawa, A. Watanabe, O. Itoh, H. Nakanishi, Chem. Lett. (1997) 1181.

[8] H. B. Fu, J. N. Yao, J. Am. Chem. Soc. 123 (2001) 1434.

[9] H. Kasai, H. S. Nalwa, H. Oikawa, S. Okada, H. Matsuda, N. Minami, A. Kakuta, K. Ono, A. Mukoh, H. Nakanishi, Jpn. J. Appl. Phys. 31 (1992) L1132.

[10] H. Kasai, H. Kamatani, S. Okada, H. Oikawa, H. Matsuda, H. Nakanishi, Jpn. J. Appl. Phys. 35 (1996) L221.

[11] S. Takahashi, H. Miura, H. Kasai, S. Okada, H. Oikawa, H. Nakanishi, J. Am. Chem. Soc. 124 (2002) 10944.

[12] R. H. Friend, R. W. Gymer, A. B. Holmes, J. H. Burroughes, R. N. Marks, C. Taliani, D. D. C. Bradley, D. A. Dos Santos, J. H. Bredas, M. Logdlund and W. R. Salaneck, Nature 397 (1999) 121.

[13] S. A. Jenekhe, J. A. Osaheni, Science 265 (1994) 765.

[14] S. Li, L. He, F. Xiong, Y. Li, G. Yang, J. Phys. Chem. B 108 (2004) 10887.

[15] C. J. Bhongale, C.-W. Chang, C.-S. Lee, E. W.-G. Diau, C.-S. Hsu, J. Phys. Chem. B 109 (2005) 13472.

[16] J. Luo, Z. Xie, J. W. Y. Lam, L. Cheng, H. Chen, C. Qiu, H. S. Kwok, X. Zhan, Y. Liu, D. Zhu, B. Z. Tang, Chem. Commun. (2001) 1740.

[17] J. Chen, C. C. W. Law, J. Y. W. Lam, Y. Dong, S. M. F. Lo, I. D. Williams, D. Zhu, B. Z. Tang, Chem. Mater. 15 (2003) 1535.

[18] J. Chen, Z. Xie, J. W. Y. Lam, C. C. W. Law, B. Z. Tang, Macromolecules 36 (2003) 1108.

[19] H. Y. Chen, W. Y. Lam, J. D. Luo, Y. L. Ho, B. Z. Tang, D. B. Zhu, M. Wong, H. S. Kwok, Appl. Phys. Lett. 81 (2002) 574.

[20] J. W. Chen, H. Peng, C. C. W. Law, Y. P. Dong, J. W. Y. Lam, I. D. Williams, B. Z. Tang, Macromolecules 36 (2003) 4319.

[21] Y. Ren, J. W. Y. Lam, Y. Dong, B. Z. Tang, K. S. Wong, J. Phys. Chem. B 109 (2005) 1135.

[22] Y. Ren, Y. Dong, J. W. Y. Lam, B. Z. Tang, K. S. Wong, Chem. Phys. Lett. 402 (2005) 468.

[23] R. Deans, J. Kim, M. R. Machacek, T. M. Swager, J. Am. Chem. Soc. 122 (2000) 8565.

[24] C. Liu, W. Yang, Y. Mo, Y. Cao, J. Chen, B. Z. Tang, Synth. Met. 135-136 (2003) 187.

[25] Y. Dong, J. W. Y. Lam, Z. Li, H. Tong, C. C. W. Law, X. D. Feng, B. Z. Tang, Poly. Mater.: Science & Engg. 91 (2004) 707.

[26] Y. Dong, J. W. Y. Lam, Z. Li, H. Peng, C. C. W. Law, X. D. Feng, B. Z. Tang, Polym. Prepr. 45 (2004) 823.

[27] Y.-Q. Zhu, W.-K. Hsu, M. Terrones, N. Grobert, W.-B. Hu, J. P. Hare, H. W. Kroto, D. R. M. Walton, Chem. Mater. 11 (1999) 2709.

[28] Y. B. Li, Y. Bando, D. Golberg, Appl. Phys. Lett. 82 (2003) 1962.

[29] C. Lu, L. Qi, J. Yang, D. Zhang, N. Wu, J. Ma, J. Phys. Chem. B 108 (2004) 17825.

[30] X. H. Sun, S. Lam, T. K. Sham, F. Heigl, A. Jurgensen, N. B. Wong, J. Phys. Chem. B 109 (2005) 3120.

[31] B. Z. Tang, X. Zhan, G. Yu, P. P. S. Lee, Y. Liu, D. Zhu, J. Mater. Chem. 11 (2001) 2974.

[32] M. H. Lee, D. Kim, Y. Dong, B. Z. Tang, J. Korean Phys. Soc. 45 (2004) 329.

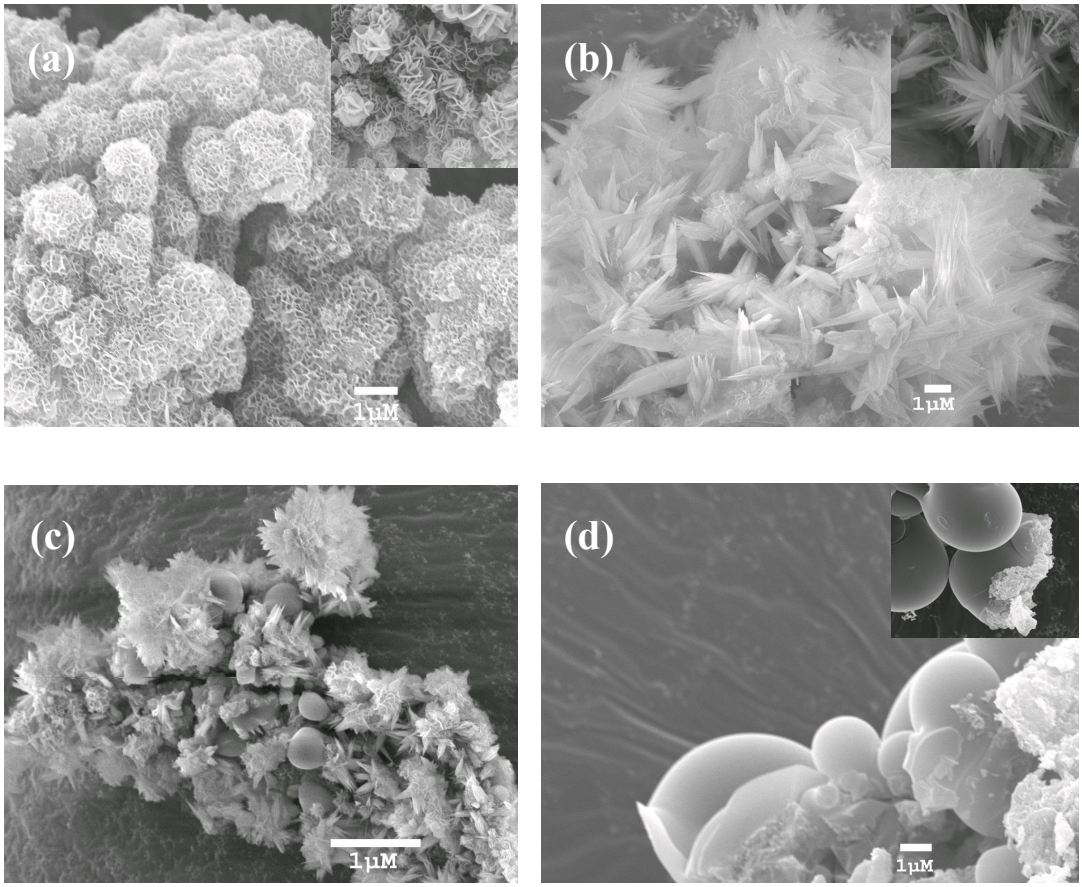

Fig. 1

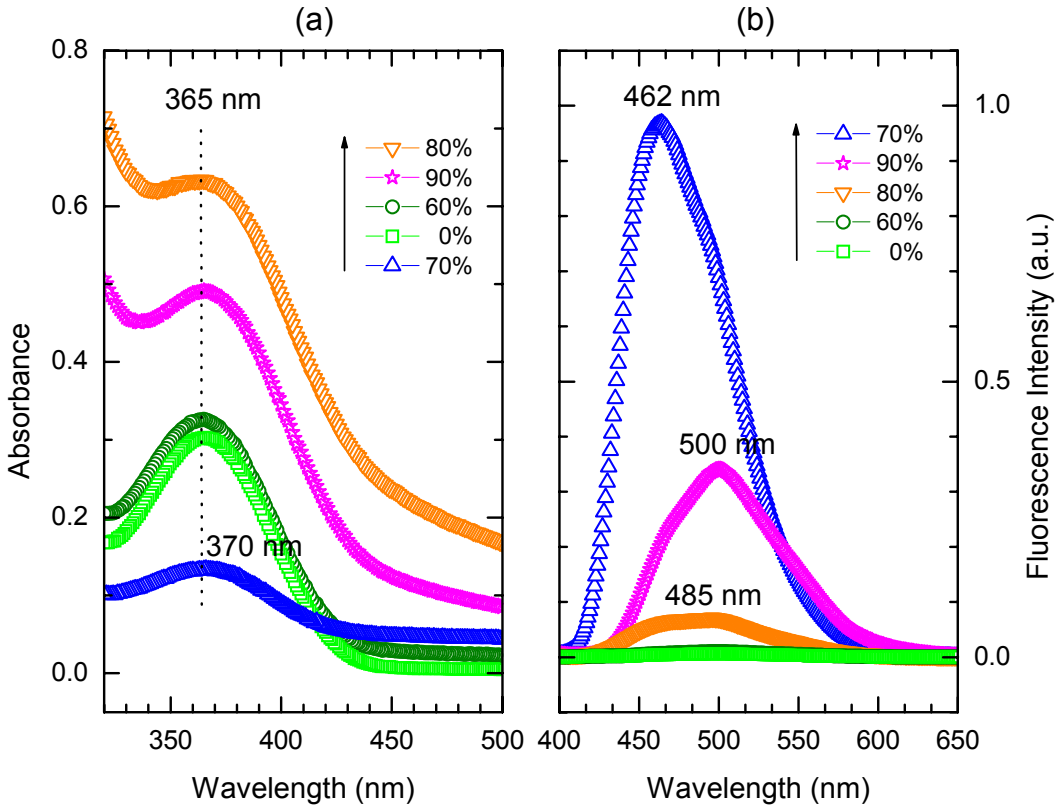
(a)
(b)
365 nm
370 nm
462 nm
500 nm
485 nm
80%
90%
60%
0%
70%
Absorbance
Fluorescence Intensity (a.u.)
Wavelength (nm)
Wavelength (nm)

Fig. 2

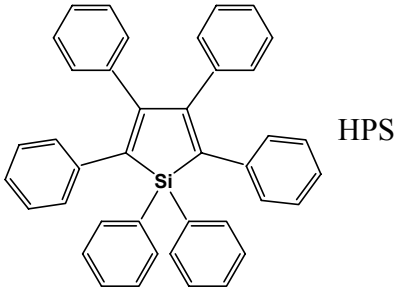

HPS

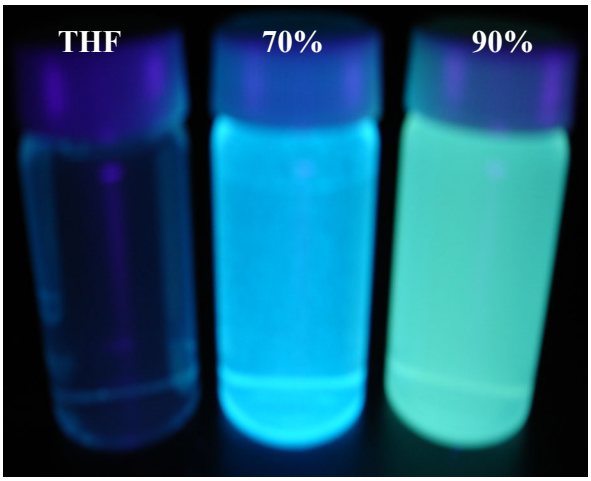

Fig. 3

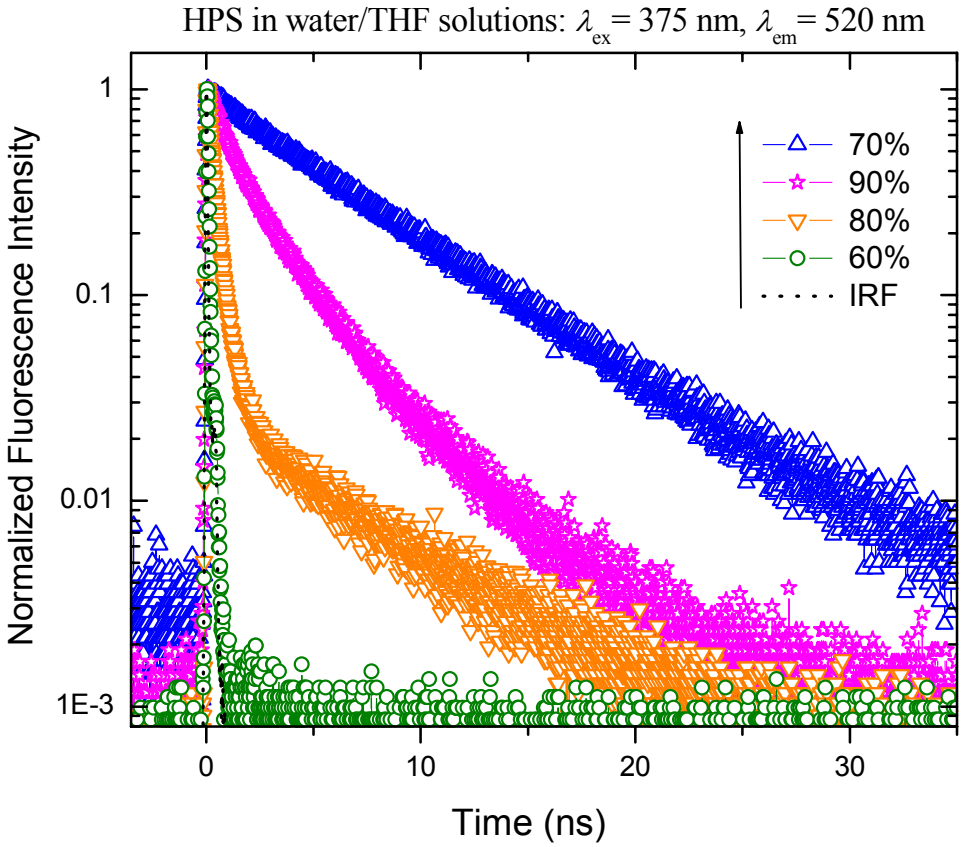
HPS in water/THF solutions: λ_{ex} = 375 nm, λ_{em} = 520 nm
Normalized Fluorescence Intensity
1
0.1
0.01
1E-3
0
10
20
30
Time (ns)
70%
90%
80%
60%
IRF

Fig. 4